ELSEVIER

Materials Science and Engineering A349 (2003) 318–326

MATERIALS SCIENCE & ENGINEERING A

www.elsevier.com/locate/msea

Fatigue life of fine-grain Al–Mg–Sc alloys produced by equal-channel angular pressing

A. Vinogradov [a,*], A. Washikita [b], K. Kitagawa [b], V.I. Kopylov [c]

[a] Department of Intelligent Materials Engineering, Osaka City University, Osaka 558-8585, Japan
[b] Department of Mechanical Systems Engineering, Kanazawa University, Kanazawa 920-5667, Japan
[c] Physical-Technical Institute of National Academy of Science of Belarus, Minsk, Belarus

Received 24 July 2002; received in revised form 15 October 2002

Abstract

The effect of severe plastic deformation through equal-channel angular pressing (ECAP) on the fatigue life of Al–Mg–Sc alloys with different concentration of magnesium is discussed. Both high-cyclic and low-cyclic fatigue properties have been assessed in terms of the fatigue strength, fatigue ductility, cyclic stress–strain curves, etc. It is shown that the addition of Sc significantly increases the thermal stability of the fine-grain structure formed during ECAP. However, only modest improvement of tensile and cyclic mechanical properties have been achieved via ECAP of Al–Mg–Sc alloys in comparison to their ordinarily fabricated counterparts. The results of present investigation show that the grain refinement of precipitation hardenable Al-alloys through severe plastic deformation can not be effective for enhancement of their static or cyclic strength. It is argued that early shear banding play an important role in cyclic degradation of ECAP Al–Mg–Sc alloys.

Keywords: Aluminium alloys; Severe plastic deformation; Fatigue

1. Introduction

The static strength, plastic and superplastic properties of aluminium alloys can benefit significantly from grain size reduction to the sub-microcrystalline scale [1,2]. The equal-channel angular pressing (ECAP) [3,4] is the technique, which allows extremely large uniform strains to be imposed through simple shear in bulk samples. During ECAP, the grain refinement occurs together with significant dislocation hardening, resulting in remarkable enhancement of mechanical parameters of many engineering materials [3–5]. The effect of ECAP on the structure, thermal stability, ductility, tensile and cyclic strength of the non-heat treatable AA5056 Al–Mg alloy manufactured by YKK Corporation, Japan has been studied previously [6]. It was shown in particular that although some increase in the tensile strength occurred after ECAP, there was no improvement in the high-cyclic fatigue (HCF) life. This was attributed to the rather low thermal and mechanical stability of the utilized Al–Mg alloy, tending to recovery and early strain localization under load. Similarly, no improvement in the low-cyclic fatigue (LCF) was observed so far in various severely deformed metals subjected to cycling under strain control [7]. It was argued that the ductility is a key factor responsible for the relatively low LCF properties of ultra-fine grained metals. Another factor affecting the fatigue life of these materials is their susceptibility to strain localization, which usually increases with increasing strain hardening and decreasing ductility. Thus, in attempt to improve the fatigue performance it is important to manage a complex combination of material properties including the strength, ductility and thermal stability. The ECAP is convenient for this purpose since it can flexibly control many processing parameters such as the number of pressings through the die, strain path, temperature, velocity, etc.

The objective of the present work is to take advantage of precipitation hardening in order to stabilize the ECAP structure and to explore the efficiency of

* Corresponding author. Tel./fax: +81-6-6605-3049.
E-mail address: alexei@imat.eng.osaka-cu.ac.jp (A. Vinogradov).

0921-5093/02/$ - see front matter
doi:10.1016/S0921-5093(02)00813-4

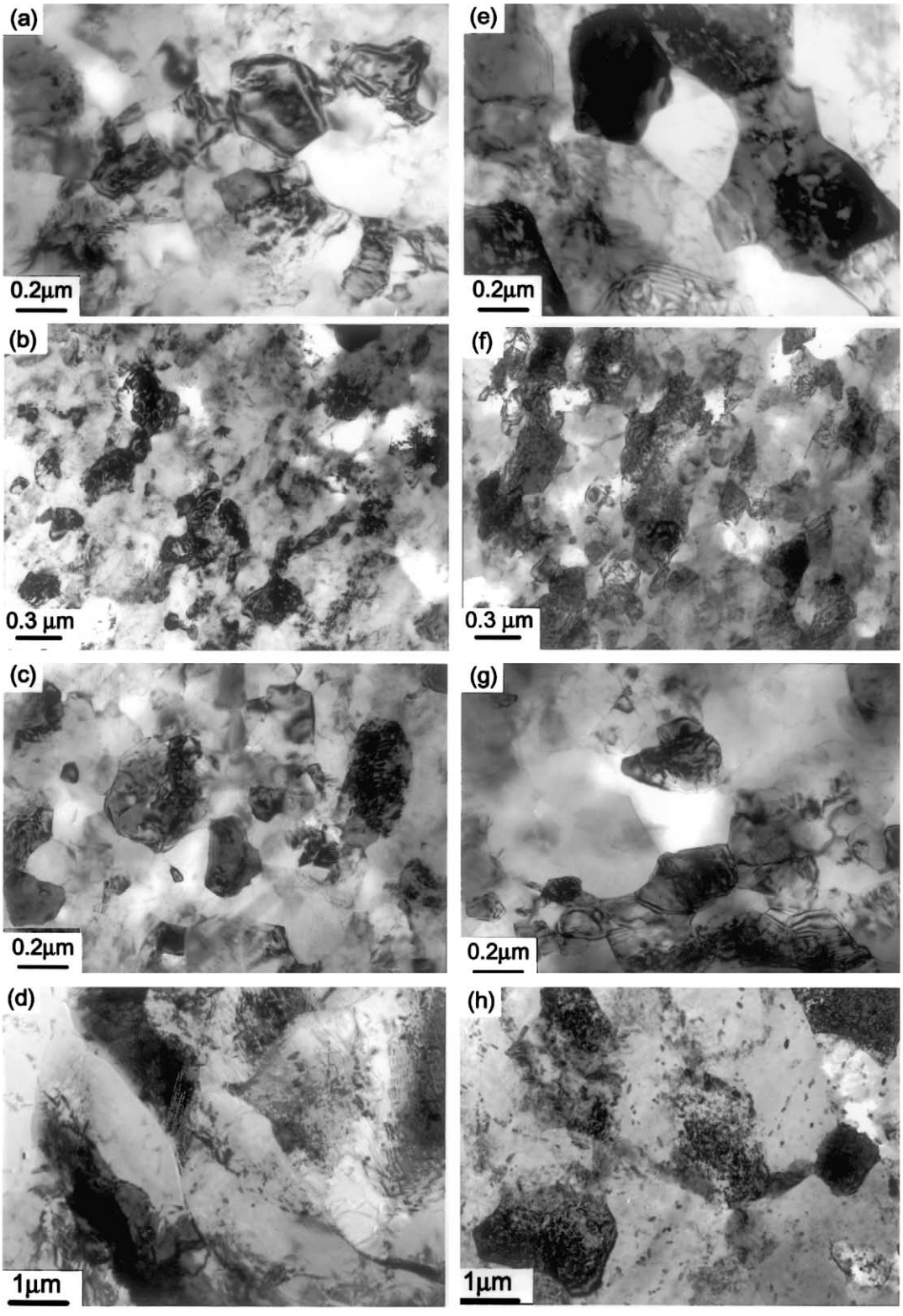

Fig. 1. TEM images showing the typical structure of Al–Mg–Sc alloys under investigation prior to (a–d) and after LCF test at $\Delta\varepsilon_{pl}/2 = 1 \times 10^{-3}$ (e–h): (a and e) Al–1.5Mg–Sc–Zr, (b and f) Al–3Mg–Sc–Zr, (c and g) Al–4.5Mg–Sc–Zr (e and h) Al–6Mg–Sc–Zr. The thin foils have been prepared from the flow plane of the ECAP billets.

Table 1
Tensile properties and fatigue limit of Al–Mg–Sc alloys

Alloy	Processing details		d (μm)	$\sigma_{0.2}$ (MPa)	σ_{UTS} (MPa)	δ (%)	σ_f (MPa)	Source
	T (°C)	N						
ECAP processing								
Al–1.5Mg–Sc–Zr	140	8	0.33	280	280	17	120	Present
Al–3.0Mg–Sc–Zr	150	6	0.26	340	360	13	135	Present
Al–4.5Mg–Sc–Zr	160	6	0.34	370	400	15	140	Present
Al–6.0Mg–Sc–Zr	320	4	12	230	410	29	150	Present
AA5056	110	8	0.28	430	450	7	110	[6]
	Temperature							
Conventional processing								
Al–6Mg–Sc–Zr	W			225	365	9	N/A	[15]
Al–5.18Mg–0.32Mn–0.25Sc	Hot rolled			240	375	29	150	[10,11]
Al–4Mg–0.3Sc	Extruded			315	415	17	160	[10]
AA5056	H18			407	434	10	152	[16]
2024	T3			325	445	18	105	[15]

The fatigue limit σ_f is based on 10^7 cycles.

precipitation hardening for fatigue life enhancement of fine and ultra-fine grain materials. We employed the model Al–Mg–Sc alloys for the present study because scandium is well known as a very efficient structure modifier forming fine coherent Al_3Sc particles in aluminium matrix [8]. These precipitates exert a complex influence on the properties of Al–Mg alloys, i.e. they significantly stabilize the grain structure and improve the strength, ductility, fatigue limit, etc. [8,9]. A high specific strength, excellent formability and weldability in combination with good corrosion resistance of Al–Mg–Sc alloys make them attractive for aircraft and marine applications. For example, the Al–Mg–Sc alloys have been considered as potential substitutes for the medium strength 2024-T3 Al-alloy for the aircraft skin [10,11]. Wirtz et al. [10] and Roder et al. [11] have shown that the fine grain Al–Mg–Sc alloys exhibit a higher resistance against fatigue crack nucleation in the HCF regime in comparison with the commercial Al–Mg–Si–Cu 6013-T6 alloy although the yield stress of Al–Mg–Sc alloys is somewhat lower than that of 6013-T6 alloy.

To date, there has been no attempt to evaluate the fatigue life of ECAP treated Al–Mg–Sc alloys and the influence of magnesium concentration on fatigue performance. Accordingly, the present experimental investigation was initiated to examine the properties of several Al–Mg–Sc alloys with equal content of Sc (0.2%) and containing different amounts of magnesium from 1.5 to 6%. The specific intention of this paper was to extend the discussion existing in the literature [2,10–12] on how the structure stabilization can help to enhance the fatigue life of sub-microcrystalline Al alloys fabricated by severe plastic deformation.

2. Experimental procedure

Four Al–Mg–Sc alloys are utilized in the present work: Al–6Mg–0.2Sc–0.15Zr, Al–4.5Mg–0.2Sc–0.2Zr, Al–3Mg–0.2Sc–0.18Zr, Al–1.5Mg–0.2Sc–0.2Zr (the concentration of elements is given in weight per cent here and further). The as-cast billets of $14 \times 15 \times 175$ mm^3 dimensions were homogenized at 460 °C for 24 h before pressing through an ECAP die having two square channels intersecting at 90° The samples having 1.5, 3 and 4.5% Mg were pressed at 150 °C while the material with 6% Mg was fabricated at about 320 °C because of its high cracking susceptibility during processing at lower temperatures. To provide the uniform simple shear rather then bending, the required boundary conditions [3–5] have been fulfilled to minimize the contact friction and to provide a hydrostatic compressive pressure in the deforming region. The uniformity of simple shear was verified after each ECA-pass by observing the fiducial lines scratched on the flow plane of the billet in the direction perpendicular to the working axis.

The mechanical testing was performed at ambient conditions using a servo-hydraulic testing machine Instron-8500. The dog-bone samples were cut by spark erosion to have a cross-section of 2×2 mm^2. The low-cycle fatigue experiments were carried out in the symmetric push–pull loading under plastic strain control with constant plastic strain amplitudes $\Delta\varepsilon_{pl}/2$ ranging from 1×10^{-4} to 1×10^{-2}. The HCF properties were evaluated under constant load amplitude cycling. The formerly obtained data for the AA5056 ECAP Al–Mg alloy (4.8Mg, 0.06Si, 0.12Si, 0.07Mn, 0.06Cr, Al-balance) are used for reference.

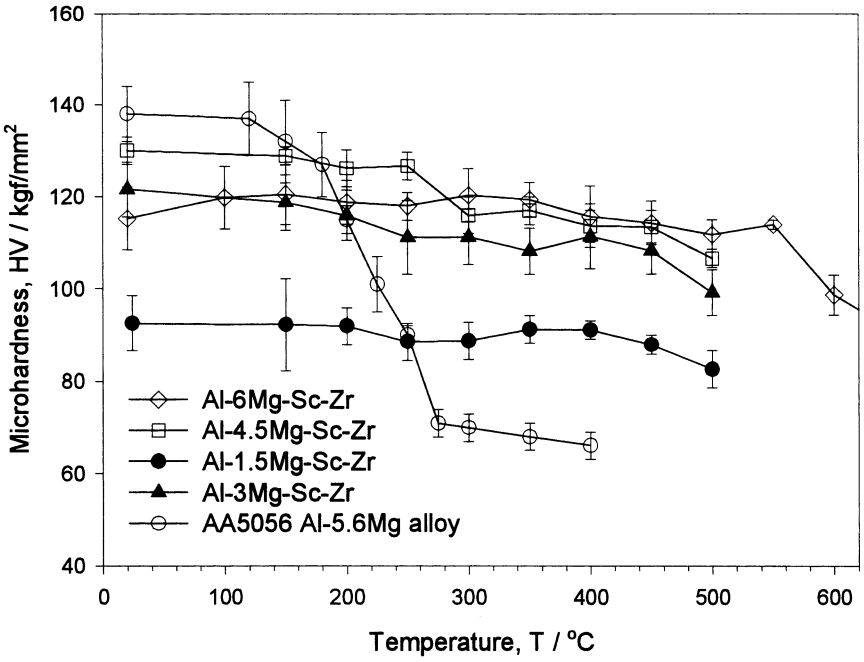

Fig. 2. Vickers microhardess plotted versus annealing temperature for different ECAP Al–Mg alloys (annealing time is 1 h).

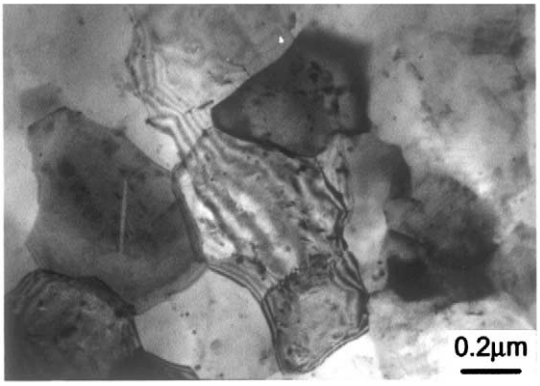

Fig. 3. TEM photo illustrating the stability of fine-grain structure of Al–4.5Mg–Sc–Zr alloy after annealing at 400 °C for 1 h.

Bright field 200 kV transmission electron microscopy (TEM) was employed for structural characterization of the samples before and after fatigue. The specimen surface after tensile and fatigue tests was observed by scanning electron microscopy (SEM).

3. Results and discussion

Representative TEM micrographs of the initial microstructure after ECAP are shown in Fig. 1(a–d). The specimens manufactured at lower temperature have a rather fine homogeneous structure with the mean grain size of 300 nm, Table 1. The pan-cake like arrangement of elongated and relatively large grains, Fig. 1d, is visible in the Al–6.0Mg–Sc–Zr samples fabricated at highest temperature. As expected, the ECAP materials containing small coherent Al_3Sc particles are rather strong while still ductile, Table 1. The restriction of grain boundary mobility owing to precipitates gives rise to enhanced thermal stability of the structure, which remains fine after annealing at temperatures as high as 500 °C. Fig. 2 shows the fine structure of the Al–4.5Mg–SC–Zr alloy after annealing at 400 °C for 1 h as an example. The other ECAP Al–Mg–Sc alloys demonstrate a high thermal stability too. Fig. 3 reveals that, in contrast to the ECAP AA5056 Al–Mg alloy, the Al–Mg–Sc alloys do not exhibit any drastic decrease in the microhardness after annealing at temperatures below 500 °C. This good thermal stability of the fine grain structure gives a hope of effective superplastic forming of ECAP Al–Mg–Sc alloys, which in fact as has been observed formerly in [13]. Additional information regarding the effect of scandium and ECAP on the structure of various engineering and model Al–Mg–Sc alloys can be found elsewhere [8,9,13,14].

During tensile deformation, the ECAP Al–Mg–Sc alloys show remarkable ductility in terms of total elongation to failure. Their ultimate tensile stress is slightly less than that of the non-heat treatable ECAP AA5056 alloy, Table 1 and Fig. 3. Furthermore, the strength of ECAP Al–Mg–Sc alloys is not much higher than that of similar materials fabricated by traditional extrusion or rolling [10,11]. This result is closely related to the discussion initiated by Markushev et al. [2] concerning the role of grain refinement by severe plastic deformation in strengthening of aluminium alloys. It has been concluded that severe plastic deformation can be

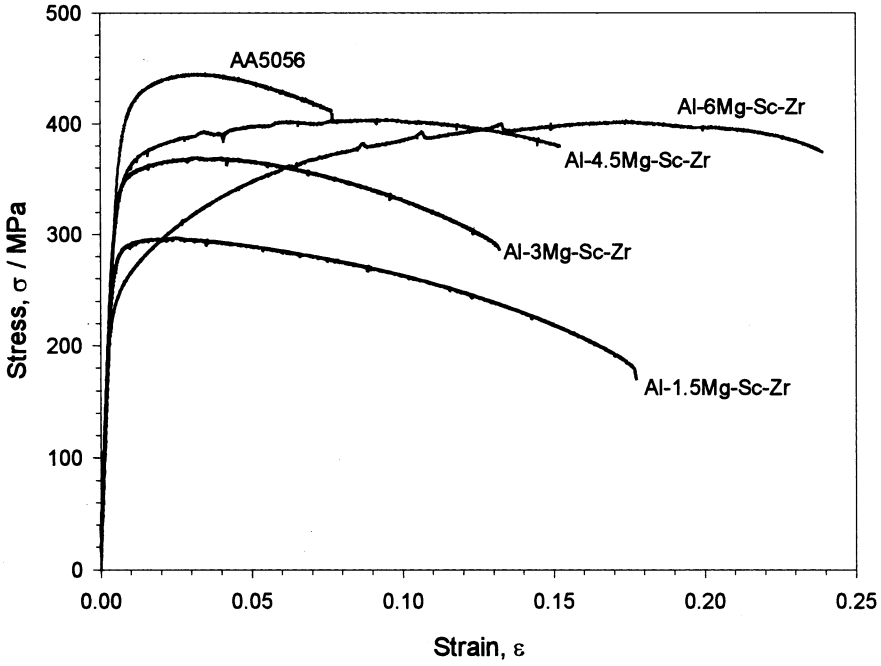

Fig. 4. Stress–strain curves for ECAP Al–Mg alloys (the strain rate is of 3×10^{-3} s^{-1}).

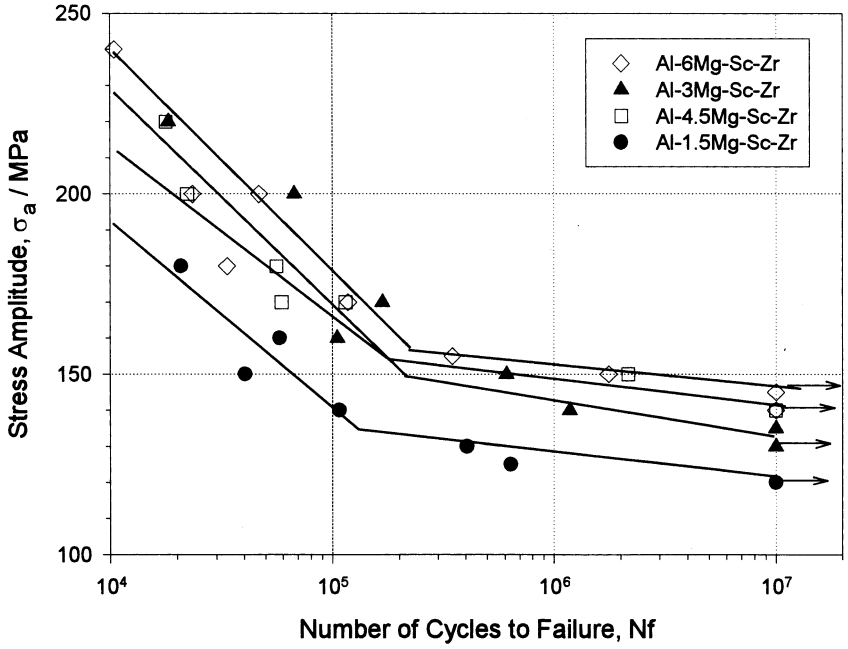

Fig. 5. HCF life displayed via Wöhler curves for Al–Mg–Sc alloys manufactured by ECAP.

helpful to obtain a unique combination of strength and ductility in non-heat treatable alloys. Our results on Al–Mg–Sc appear to be in line with former findings reported for other precipitation hardened Al alloys [10–12], i.e. the static strength improvement is modest while the ductility gain in notable.

The ECAP materials do not reveal significant strain hardening during monotonic deformation, Fig. 4, except the relatively coarse-grain Al–6.0Mg–Sc–Zr alloy. The gradual stress decrease upon straining should be associated with strain localization and will be discussed below.

Table 1 compares the fatigue and tensile properties of the ECAP materials studied. Properties of some other Al–Mg–Sc alloys and commercial 2024-T3 Al-alloy are given for comparison. The S–N plot characterizing the fatigue life under testing at constant load amplitude is shown in Fig. 5. The S–N curve does not show an

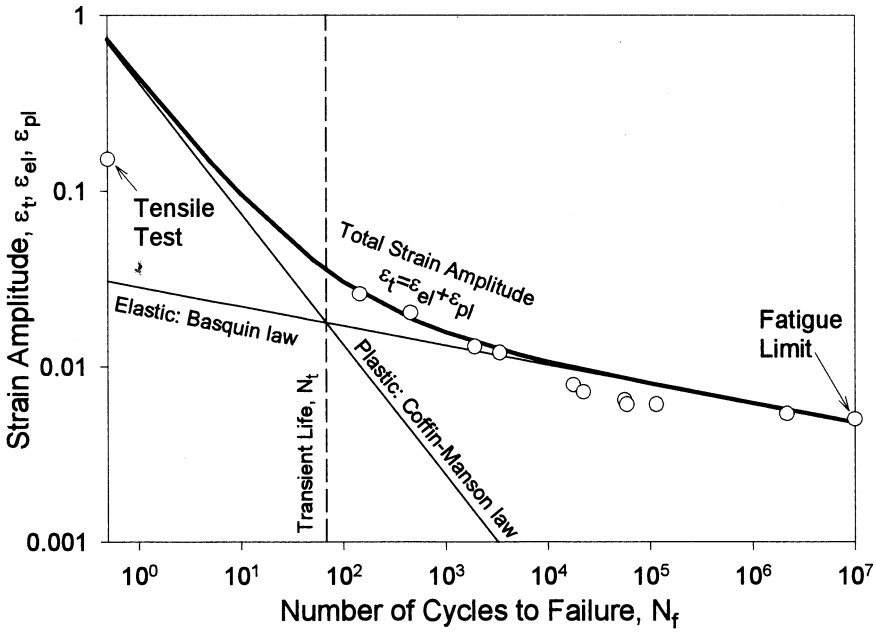

Fig. 7. A total strain fatigue life diagram for Al–4.5Mg–Sc–Zr alloy.

Table 2
Fatigue life related parameters of ECAP Al–Mg–Sc alloys

ECAP alloy	ε_f'	c	σ_f'/E	b	σ_f (MPa)	$2N_t$
Al–1.5Mg–Sc–Zr	0.86	−0.72	0.0018	−0.074	120	390
Al–3.0Mg–Sc–Zr	0.79	−0.79	0.0237	−0.095	135	155
Al–4.5Mg–Sc–Zr	0.70	−0.74	0.0307	−0.110	140	145
Al–6.0Mg–Sc–Zr	1.28	−0.81	0.0272	−0.089	145	210
AA5056	1.61	−0.86	0.0181	−0.068	110	290

apparent knee and the fatigue limit, σ_f, is not well defined, which is typical of many aluminium alloys. Therefore, the conventional fatigue limit based on 10^7 cycles (called further as fatigue strength) was measured and served as a measure of HCF life. One can see that, in line with general expectations [17,18], the fatigue strength increases with increasing ultimate tensile strength, σ_{UTS}, and magnesium content. However, this is not the case for the non-heat treatable AA5056 Al–Mg alloy where no enhancement in fatigue strength has been observed after ECAP if compared with its ordinary commercial analogue. Furthermore, despite the somewhat lower tensile strength, the fatigue strength of Al–Mg–Sc alloys is apparently higher than that of the ECAP AA5056 alloy and the commercial precipitation hardened 2024-T3 alloy.

While the fatigue limit (or fatigue strength for materials which do not show an apparent fatigue limit) serves as an appropriate measure of materials reliability for practical applications where the part works in the non-constrained mode, in many situations the material experiences some extent of plastic deformation. For later situation, a total strain approach to the fatigue life applies naturally [17]. The total strain range $\Delta\varepsilon_t$ consists of two components—the elastic $\Delta\varepsilon_{el}$ and plastic $\Delta\varepsilon_{pl}$. The empirical Coffin–Manson law relates the total fatigue life (number of cycles to failure N_f) to the plastic strain amplitude $\Delta\varepsilon_{pl}/2$ as:

$$\frac{\Delta\varepsilon_{pl}}{2} = \varepsilon_f'(2N_f)^c \quad (1)$$

where ε_f' is the fatigue ductility coefficient and c is the fatigue ductility exponent. The elastic strain amplitude $\Delta\varepsilon_{el}/2$ is given as:

$$\frac{\Delta\varepsilon_{el}}{2} = \frac{\Delta\sigma}{2E} \quad (2)$$

where E is the Young's modulus and $\Delta\sigma$ is the stress amplitude range. Thus, using the Basquin expression relating the stress amplitude to the total number of reversals to failure $2N_f$ as:

$$\frac{\Delta\sigma}{2} = \sigma_f'(2N_f)^b \quad (3)$$

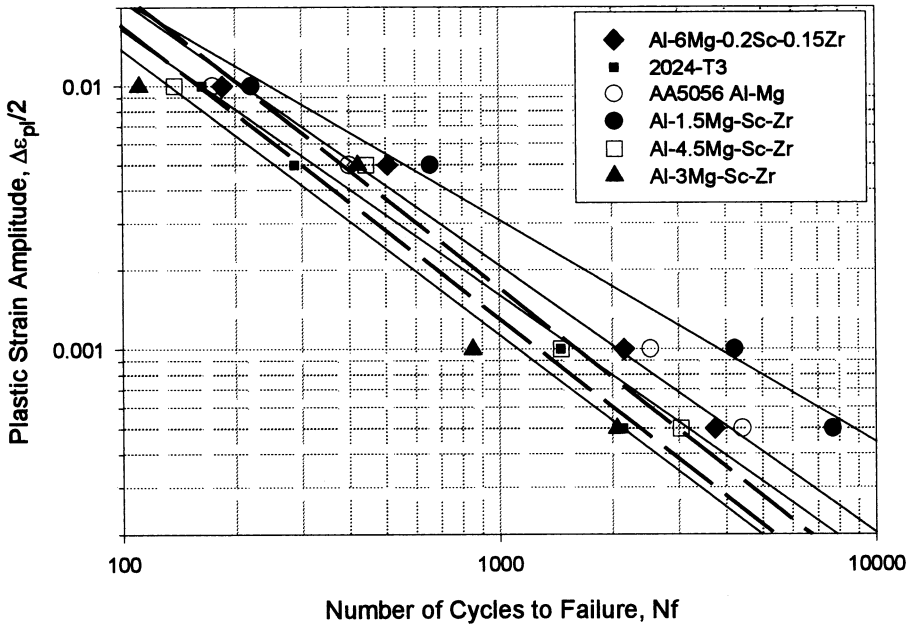

Fig. 6. Coffin–Manson plot for Al–Mg–Sc alloys manufactured by ECAP. Data for 2024-T3 and ECAP 5056 Al alloys are plotted for comparison.

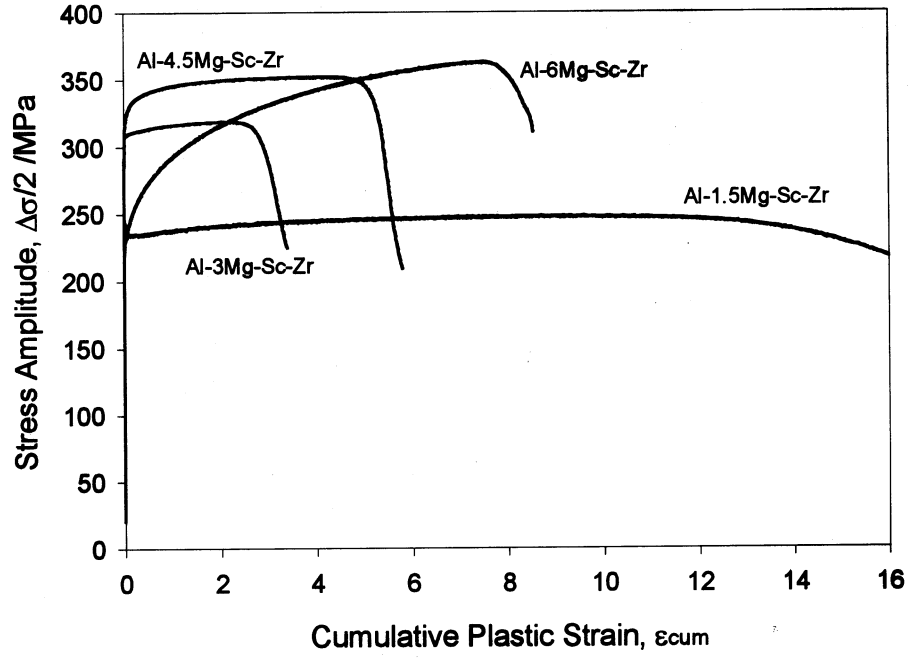

Fig. 8. Cyclic hardening curves for Al–Mg–Sc–Zr alloys, $\Delta\varepsilon_{pl}/2 = 1 \times 10^{-3}$.

one obtains the elastic strain component:

$$\frac{\Delta\varepsilon_{el}}{2} = \sigma'_f(2N_f)^b \quad (4)$$

Combining the Eqs. (1) and (4), the fatigue life under a given total strain is expressed in terms of materials constants:

$$\frac{\Delta\varepsilon_t}{2} = \sigma'_f(2N_f)^b + \varepsilon'_f(2N_f)^c \quad (5)$$

It follows from Eq. (5) that at short lives, the plastic strain component is dominant and the fatigue life is determined by ductility. At long fatigue lives, the elastic strain amplitude is more significant and the fatigue life is dictated by the fracture strength so that the fatigue limit (strength) increases with monotonic strength. Taking experimental data for the saturation regime of plastic strain controlled cyclic tests and applying an approximation procedure separately to elastic and plastic components of hysteresis loops we can obtain the above

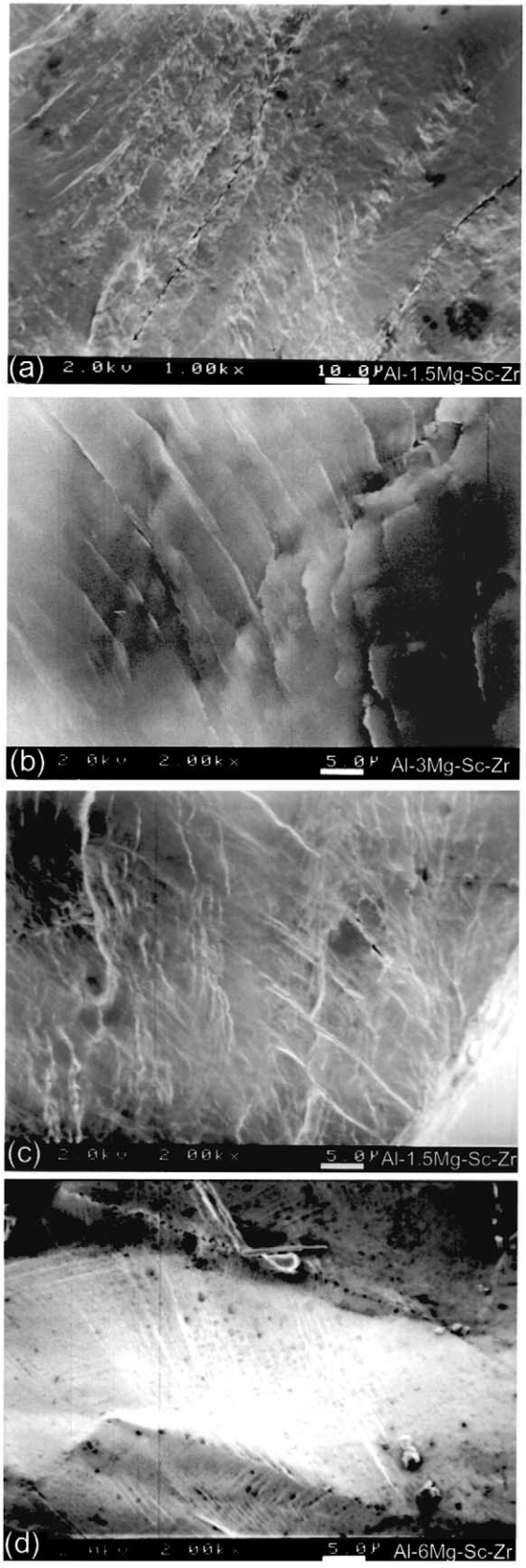

Fig. 9.

mentioned parameters σ_f', b, ε_f' and c. Fig. 7 illustrates this approach for the ECAP alloy containing 4.5% Mg. The fatigue life parameters for all specimens are summarized in Table 2. The so-called transient life N_t is defined as the number of cycles to failure when the amplitudes of elastic and plastic components are equal:

$$N_t = \left[\frac{\varepsilon_f' E}{\sigma_f'}\right]^{1/(b-c)} \quad (6)$$

Thus N_t separates the 'short' and 'long' fatigue lives and the decreasing N_t magnitude corresponds usually to the reducing LCF life [18]. As underlined in [17,18] the resistance to cracking can be assessed directly by measuring the crack growth rate in the notched bodies subjected to cyclic loading under different stress–strain conditions or indirectly by using the LCF data. The average values of fatigue life parameters (Table 2) appear within a range of magnitudes common for many engineering Al-alloys produced by conventional techniques [18]. Table 2 demonstrates that a reasonable compromise between the strength and ductility can be achieved by varying the magnesium content and processing conditions.

From the Coffin–Manson plot, Fig. 6, and the cyclic hardening curves, Fig. 8, it is apparent that the LCF fatigue properties of ECAP Al–Mg–Sc alloys depend on magnesium content. Figs. 5, 6 and 8 show that as long as cyclic durability is of major concern it is not necessary to pay a high price for obtaining the finest possible grain size in precipitation hardened Al-alloys: the longer fatigue life is observed in the specimen manufactured at relatively high temperature and thus having relatively large grain size. Besides, this specimen exhibits the highest fatigue limit in the high-cyclic regime, Table 1 and Fig. 4, demonstrating thereby an excellent overall performance if assessed in terms of ultimate strength, ductility and fatigue life in combination with good thermal stability (for the cyclic response and fracture behavior of the ECAP Al–6Mg–Sc–Zr alloy see also [17] where the significant local ductility is emphasized from fracture surface observations).

The absence of strain hardening is known as a precursor to possible plastic instabilities which occur in many severely deformed materials in a form of shear bands during either monotonic or cyclic straining [7]. The ECAP Al–Mg–Sc alloys are prone to intensive shear banding in the same manner as in many other ECAP materials. The shear bands appear at about 45° to the loading axis and are aligned with the shear plane of the last ECA-pass, Fig. 9. The density of shear bands increases somewhat with increasing Mg concentration in

Fig. 9. SEM micrographs showing the appearance of shear bands on the surface of cyclically tested ECAP Al–Mg–Sc alloys ($\Delta\varepsilon_{pl}/2 = 1 \times 10^{-3}$): (a) Al–1.5Mg–Sc–Zr; (b) Al–3Mg–Sc–Zr; (c) Al–4.5Mg–Sc–Zr and (d) Al–6Mg–Sc–Zr.

the fine-grained Al–Mg–Sc alloys. Visible traces of plastic deformation in the Al–6Mg–Sc–Zr specimens are limited to the grain size. Their orientation with respect to the loading axis varies form grain to grain similarly to a dislocation slip in ordinary polycrystalline materials. According to their appearance the slip markings in the Al–6Mg–Sc–Zr alloy should be associated with the coarse slip bands rather than with the shear bands, which are notably longer than the grain diameter and oriented at 45° to the specimen axis. Fig. 4 illustrates that pronounced strain hardening takes place in the Al–6Mg–Sc–Zr sample in contrast to the fine-grain specimens. In other words, it seems evident that ordinary dislocation mechanisms are responsible for the mechanical behavior of the Al–6Mg–Sc–Zr alloy manufactured at elevated temperature whereas the large-scale plastic instability and strain localization influence significantly the tensile and fatigue performance of fine-grain ECAP Al–Mg–Sc alloys manufactured at lower temperatures. We should emphasize that despite the somewhat lower yield stress, the specimen, which is least susceptible to strain localization, demonstrates a rather good overall fatigue performance and ductility. Besides, many examples show that failure occurs in ECAP materials including Al–Mg–Sc alloys primarily along the shear bands [7]. Therefore, it seems plausible to conclude that namely due to plastic instabilities the cyclic properties appear lower than expected. Although macroscopic strain localization in the shear bands does occur in the course of monotonic or cyclic straining of fine-grain ECAP Al–Mg–Sc alloys, it does not lead to immediate fracture. This evidences for the quite good microscopic ductility in these materials, which helps to relief local internal stresses around the shear bands, delaying crack initiation and defending against crack propagation. Among other materials investigated in the present work, the Al–6Mg–Sc–Zr alloy manufactured at elevated temperature possesses the best potential for further strengthening through conventional rolling or other thermo-mechanical treatment. In this sense, in the present work we have demonstrated the possibility to obtain semi-finished Al-based products having considerable resources for deformation processing after ECAP.

4. Summary

The addition of scandium in Al–Mg alloys stabilizes significantly the fine-grain structure formed during ECAP. Variation of magnesium content and processing conditions provides extra flexibility for materials design allowing us to make a judicious choice between the relatively high strength, ductility and fatigue performance, depending on anticipated applications. The observed combination of high strength and ductility gives a hope for obtaining the Al–Mg–Sc articles with enhanced fatigue properties in both HCF and LCF regimes. However, one should bear in mind that only the modest enhancement of tensile and cyclic mechanical properties has been achieved after ECAP of Al–Mg–Sc alloys in comparison with their ordinarily fabricated counterparts. It is argued that plastic instabilities play an important role in cyclic degradation of ECAP Al-alloys and can be largely responsible for premature failure of materials fine grained by ECAP. Because of the relatively high cost of materials manufacturing via severe plastic deformation some doubts arise on the merit of grain refinement in precipitation hardenable Al-alloys if the enhancement of their static or cyclic strength is of primary concern.

Acknowledgements

Special thanks are due to Dr V. Patlan for experimental assistance and useful discussions.

References

[1] M. Furukawa, Z. Horita, T.G. Langdon, Adv. Eng. Mater. 3 (2001) 121.
[2] M.V. Markushev, C.C. Bampton, M.Y. Murshkin, D.A. Hardwick, Mater. Sci. Eng. A234–236 (1997) 927.
[3] V.M. Segal, Mater. Sci. Eng. A197 (1995) 157.
[4] V.M. Segal, V.I. Reznikov, V.I. Kopylov, D.A. Pavlik, V.F. Malyshev, Processes of Plastic Structure Formation of Metals (In Russian), Nauka i Tehnika, Minsk, 1994, p. 232.
[5] V.I. Kopylov, in: T.C. Lowe, R.Z. Valiev (Eds.), Investigations and Applications of Severe Plastic Deformation, NATO ASI Series 3, vol. 80, Kluwer, The Netherlands, 2000, p. 23.
[6] V. Patlan, A. Vinogradov, K. Higashi, K. Kitagawa, Mater. Sci. Eng. A300 (2001) 171.
[7] A. Vinogradov, S. Hashimoto, Mater. Trans. JIM 42 (2001) 74.
[8] Y.A. Filatov, V.I. Yelagin, V.V. Zakharov, Mater. Sci. Eng. A280 (2000) 97.
[9] Y.A. Filatov, J. Adv. Mater. 2 (1995) 386.
[10] T. Wirtz, G. Lütejering, A. Gysler, B. Lenczowski, R. Rauh, Mater. Sci. Forum. 331–337 (2000) 1489.
[11] O. Roder, T. Wirtz, A. Gysler, G. Lütejering, Mater. Sci. Eng. A234–236 (1997) 181.
[12] M.V. Markushev, M.Y. Murashkin, Phys. Metals Metallogr. 90 (2000) 506.
[13] M. Furukawa, A. Utsunomiya, K. Matsubara, Z. Horita, T.G. Langdon, Acta Mater. 49 (2001) 3829.
[14] H. Akamatsu, T. Fujinami, Z. Horita, T.G. Langdon, Scripta Mater. 44 (2001) 759.
[15] A. Washikita, K. Kitagawa, V.I. Kopylov, A. Vinogradov, in: Y.T. Zhu, T.G. Langdon, R.S. Mishra, S.L. Semiatin, M.J. Saran, T.C. Lou (Eds.), Ultrafine grain metals II, TMS (2002) 341.
[16] Metals Handbook, vol. 2, ASM, Metal Park, OH, USA, 1979, p. 856.
[17] S. Suresh, Fatigue of Materials, Cambridge University Press, UK, 1991, p. 617.
[18] J. Polák, Cyclic Plasticity and Low Cycle Fatigue Life of Metals, Elsevier, The Netherlands, 1991, p. 315.